PROCEEDINGS OF SPIE

SPIEDigitalLibrary.org/conference-proceedings-of-spie

Modeling, fabrication, and readout of compact optomechanical accelerometers

Brina Martinez, Andrea Nelson, Adam Hines, Jonathan Mock, Guillermo Valdés, et al.

Brina B. Martinez, Andrea Nelson, Adam Hines, Jonathan P. Mock, Guillermo Valdés, Jose Sanjuan, Felipe Guzmán, "Modeling, fabrication, and readout of compact optomechanical accelerometers," Proc. SPIE 12434, MOEMS and Miniaturized Systems XXII, 1243404 (15 March 2023); doi: 10.1117/12.2655490

SPIE.

Event: SPIE OPTO, 2023, San Francisco, California, United States

Modeling, fabrication, and readout of compact optomechanical accelerometers

Brina B. Martinez[a], Andrea Nelson[a,b], Adam Hines[a], Jonathan P. Mock[a], Guillermo Valdés[a], Jose Sanjuan[a], and Felipe Guzmán[a]

[a]Texas A&M University, College Station, Texas, USA
[b]The University of Arizona, Tucson, Arizona, USA

ABSTRACT

High-sensitivity accelerometers are key for many applications including ground-based gravitational wave (GW) detectors, in-situ or satellite gravimetry measurements, and inertial navigation systems. We will present our work on the development of optomechanical accelerometers based on the micro-fabrication of mechanical resonators and their integration with laser interferometers to read out their test mass dynamics under the presence of external accelerations. We will discuss the latest developments on compact millimeter-scale resonators made of fused silica and silicon, optimized for frequencies below 1 kHz and exhibiting low mechanical losses. While fused silica has demonstrated high mechanical quality factors at room temperature, silicon devices perform significantly better at very low temperatures, which is particularly relevant for future ground-based gravitational wave detectors where cryogenic environments will be used to improve the sensitivity of the observatories. We will report on our design, modeling, and fabrication process for the silicon-based resonators and present their characterization by means of highly compact fiber-based Fabry-Perot cavities.

Keywords: Fabrication, Optomechanics, Inertial Sensor, Accelerometer, Resonator

1. INTRODUCTION

Inertial sensors and accelerometers play an important role in fields such as inertial navigation (to estimate trajectories from acceleration measurements), ground-based gravitational wave detectors[1] (to measure and subtract seismic noise), and gravimetry (to measure and correct for non-gravitational forces in spacecraft or airplanes gravimetry), among others. Current gravimeters, accelerometers, and seismometers are large, costly, and incompatible with vacuum environments. Consequently, their accommodation and installation in many applications become complicated, or simply impossible. In addition, current seismometers are incompatible with cryogenic temperatures, which future ground-based gravitational wave detectors plan to operate at.[2] Optomechanical accelerometer performance is ultimately limited by thermal noise caused by the resonator itself,[3] which is strongly related to the mechanical losses of the material, i.e., the so-called quality factor, Q. Silicon has shown a much higher quality factor at cryogenic temperatures than fused silica,[4] which suggests its use for accelerometers working at cryogenic temperatures. In this paper, we present the current status of the fabrication and characterization of compact silicon resonators, together with potential optical read-outs using fiber-based Fabry-Pérot cavities.

2. MECHANICAL RESONATORS

The resonator is a key element of the accelerometer since it is the one in charge to sense the external accelerations and convert them to displacements, which are measured by optical means. Displacement is converted to acceleration as $\delta a = \omega_0^2 \delta x$ (for frequencies below ω_0), where ω_0 is the natural angular frequency of the resonator. High resonance frequency implies larger bandwidth but lower sensitivity, and vice versa. In the following, we discuss two resonator designs exhibiting different resonance frequencies.

The first design is a compact variation of the monolithic folded pendulum based on the Watt-linkage geometry[5,6] under gravitational restoring force, which was adjusted into an inertial sensor[7,8] by placing the flexures

Further author information: (Send correspondence to B.B.M. : E-mail: brinamartinez@tamu.edu)

MOEMS and Miniaturized Systems XXII, edited by Hans Zappe, Wibool Piyawattanametha, Yong-Hwa Park, Proc. of SPIE Vol. 12434, 1243404 · © 2023 SPIE
0277-786X · doi: 10.1117/12.2655490

closer together. Our version of the pendulum resonator, seen in Figure 1a, is roughly 30 mm×30 mm in size with a thickness of 380 μm and a theoretical fundamental frequency of 52 Hz. The second design, known as the parallelogram resonator, is a millimeter scale variation of a fully monolithic optomechanical accelerometer developed by Guzman et al.[9] Our compact version, shown in Figure 1b, is roughly 15 mm×10 mm in size with a thickness of 280 μm[10,11] and a theoretical fundamental frequency of about 1 kHz.

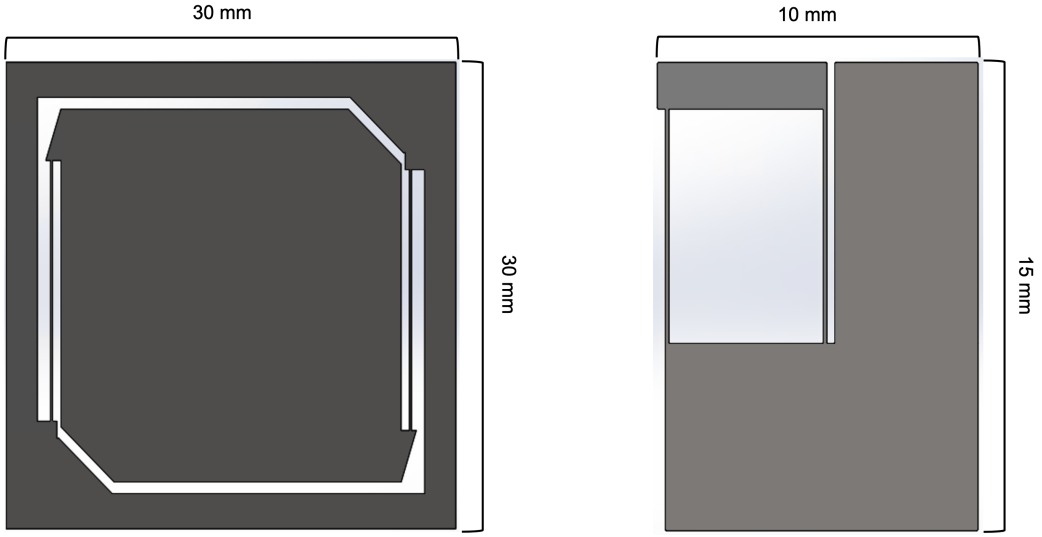

(a) (b)

Figure 1: Monolithic model designs of resonators. (a) A 30 mm×30 mm×380 μm model with a theoretical fundamental frequency of 52.4 Hz, named folded pendulum resonator, and (b) a 15 mm×10 mm×280 μm model with a theoretical fundamental frequency of 1 kHz, named parallelogram resonator.

Their material and size allow them to be compatible with compact spacecraft used in geodesy, compatible with vacuum environments, and with cryogenic temperatures (10 K -20 K) foreseen in future gravitational-wave detectors.[2,12]

2.1 Material choice

The two materials we develop the resonators in are fused silica and silicon. Fused silica has demonstrated high mechanical quality factors (Q) at room temperatures. The Q at room temperature is around 10^7. However, at 110 K it has drop to 10^4, and at cryogenic temperatures ($\sim$20 K) it is only around 10^3.[13] Current gravitational wave detectors operate at room temperature, however, future detectors will operate at cryogenic temperatures, roughly at or below 20 K,[2,12] to minimize thermal noise. To achieve a high Q-factor and, thus, high sensitivity by reducing the thermal noise limit, resonators operated at cryogenic temperatures will be fabricated from materials other than fused silica. Silicon has demonstrated a high Q-factor across both room and cryogenic temperatures. The value from 10 K to room temperature is between 10^7 and 10^8.[4,13]

Thus, the mechanical Q-factor of silicon is roughly 5 orders of magnitude higher than the fused silica one,[4] making this material an ideal candidate for operating at cryogenic temperatures. We have designed and fabricated two compact resonators, see Figure 1, from silicon that will aim to operate at high sensitivities, while overcoming the issues fused silica faces at cryogenic temperatures.

2.2 Design and modeling

The motion, fundamental frequency, and higher-order modes of oscillation are determined by the characteristics of the design such as the size of the test mass, the thickness of the sample, and the position and length of the flexures. Resonator models are developed using multiphysics software such as Solidworks and COMSOL. When a design is drafted, linear static and modal simulations are run on the models using loads such as gravity and

applied fixed geometry to estimate the fundamental mode as shown in Figure 2 and stress on the resonator to ensure physical integrity.

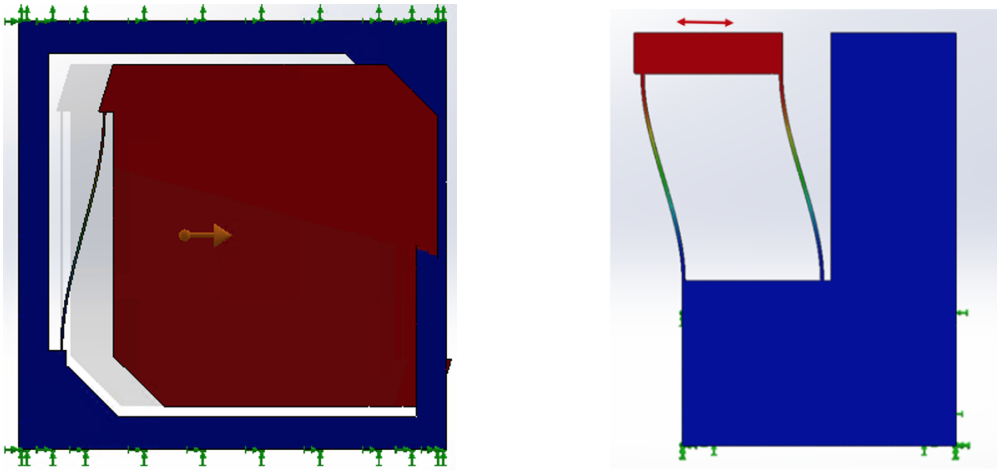

(a) (b)

Figure 2: Fundamental mode motion of our (a) folded pendulum resonator model and (b) parallelogram resonator model.

For the pendulum model, fundamental mode geometry shows $\omega_0/2\pi$ around 52.44 Hz with higher order modes varying on the thickness of the silicon wafer. For a 380 μm-thick wafer, the fundamental and higher mode frequencies are shown in Table 1. Large separations between the fundamental and higher-order modes are important for preventing cross-talks between them. The entire mass of the 380 μm-thick model structure is 0.71 g, while the test mass is 0.47 g. A larger test mass allows for better sensitivity due to the inverse relationship between the thermal acceleration noise floor and the mQ product of the resonator.[3]

Table 1: Theoretical fundamental and higher order modes of the pendulum resonator.

Fundamental Mode	52.4 Hz
2nd Mode	98.6 Hz
3rd Mode	134.5 Hz
4th Mode	252.2 Hz
5th Mode	3.2 kHz

For the parallelogram model, the fundamental frequency, $\omega_0/2\pi$, is around 1 kHz. High-order modes are shown in Table 2 for a thickness of 280 μm The entire mass of the 280 μm model structure is 72.5 mg and the test mass is about 5.4 mg.

Table 2: Theoretical fundamental and higher order modes of the parallelogram resonator.

fundamental Mode	1 kHz
2nd Mode	1.1 kHz
3rd Mode	3.6 kHz
4th Mode	3.8 kHz
5th Mode	14.9 kHz

Using the ω_0 and test mass information we gathered from the theoretical designs, we can calculate the expected linear spectral density of displacement and acceleration thermal noise floors[3] at the cryogenic temperature of 20 K and in vacuum. We calculate the effects from the thermoelastic, surface, and bulk loss mechanisms. The results of the calculations are shown in Figure 3 for the pendulum resonator and Figure 4 for the parallelogram resonator.

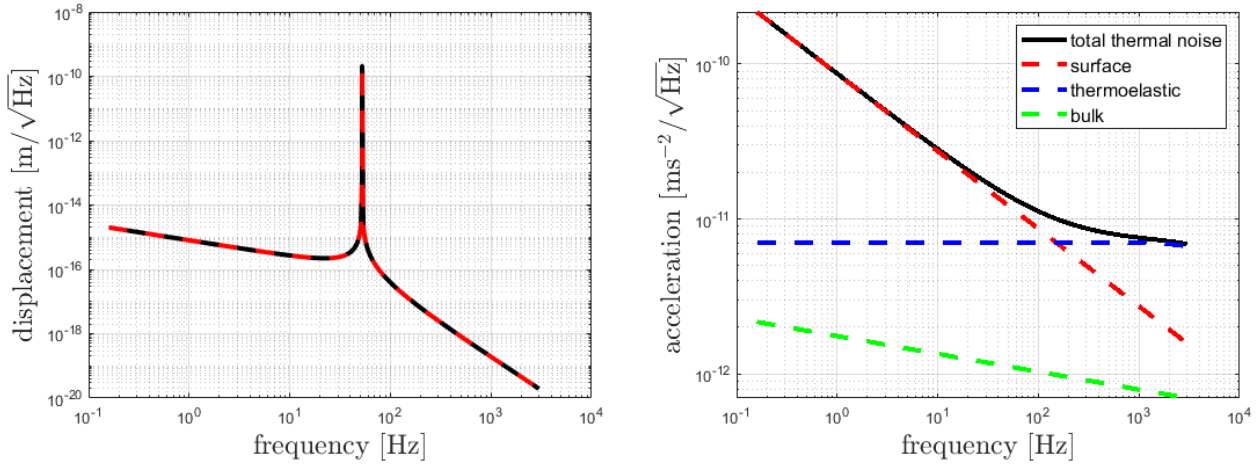

(a) (b)

Figure 3: (a) Calculated expected linear spectral density of displacement thermal noise floor for a 52.4 Hz, 0.47 g test mass at the cryogenic temperature of 20 K and in vacuum. and (b) Calculated expected linear spectral density of acceleration thermal noise for a 52.44 Hz, 0.47 g test mass at the cryogenic temperature of 20 K and in vacuum. Also plotted are the contributions from each loss mechanism, from which we can see that thermoelastic damping losses are the dominant noise source for frequencies below resonance. The theoretical Q-value for this design is 4.3×10^5.

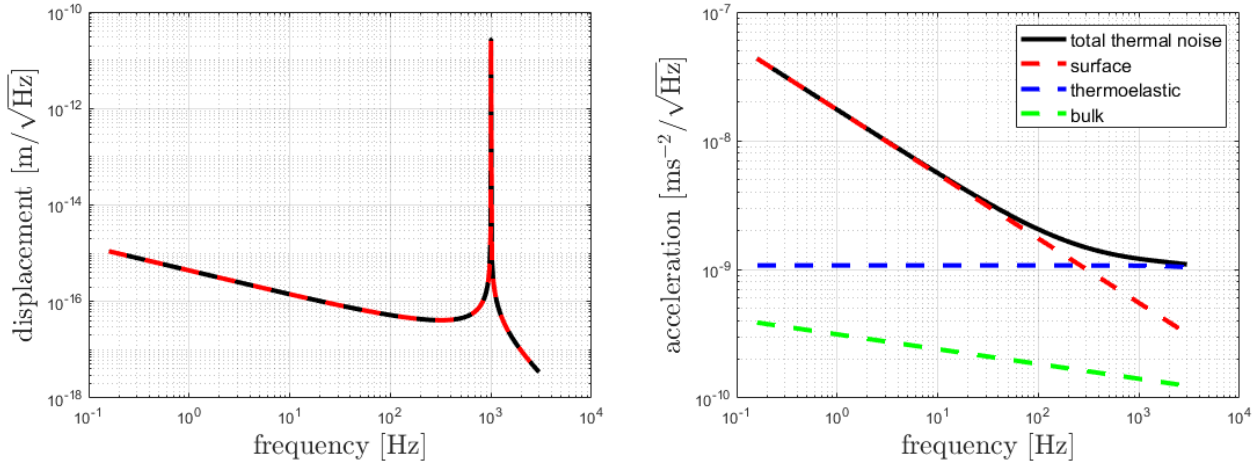

(a) (b)

Figure 4: (a) Calculated expected linear spectral density of displacement thermal noise floor for a 1 kHz, 5.4 mg test mass at the cryogenic temperature of 20 K and in vacuum. and (b) Calculated expected linear spectral density of acceleration thermal noise for a 1 kHz, 5.4 mg test mass at the cryogenic temperature of 20 K and in vacuum. Also plotted are the contributions from each loss mechanism, from which we can see that thermoelastic damping losses are the dominant noise source for frequencies below resonance. The theoretical Q-value for this design is 3.1×10^5

3. SILICON RESONATOR FABRICATION

At Texas A&M University's AggieFab Nanofabrication Facility, we fabricate resonators made of silicon. We use the processes of deposition, photolithography, and plasma "dry" etching to fabricate them. The resonator designs are printed on a soda-lime photomask to be used in a contact mask aligner. Silicon wafers are available in a variety of sizes. We currently focus on wafers with thicknesses of 280 μm, 380 μm, and 500 μm. Our current etch technique, the Cryo-Si etch, has not been optimized enough to be able to process wafers thicker than 500 μm. Any thickness below 280 μm will cross-couple the resonant and higher order modes too closely due to the reduced size of the test mass and overall structure.

3.1 Fabrication steps

In the following, we describe the main steps in the fabrication process. First, the wafer is cut down to fit the size of the resonator that will be developed. Second, the wafer is cleaned and the silicon is coated in a thin layer of aluminum via E-beam deposition. The aluminum will act as a selective hard mask to protect the un-exposed silicon beneath it during the final etch. In the next step, a positive photo-resist is applied and spread out evenly onto the layer of aluminum via a spin coater. The layer of photoresist will be used as the stamping layer between the photo mask and substrate. Subsequently, the pattern is transferred from the photo mask onto the photo-resist layer using photo-lithography via an EVG 610 double-sided mask aligner. Finally, Deep Reactive Ion Etching (DRIE) is used to etch our pattern via an Oxford Plasmalab 100 ICP RIE system using SF_6 and O_2 gas.

Two 1 kHz parallelogram resonators have been successfully etched and cleaned from a 280 μm wafer via the cryo-Si method, shown in Figure 5. The process for incorporating the etching of the v-grooves onto the test mass of the kHz resonator is currently ongoing. To create the v-grooves onto the structure we will be using a KOH etch along the surface of the silicon wafer, this is a wet etch technique that will have to be done before fabricating the rest of the resonator. Si_3N_4 or SiO_2 will be used as a mask to protect the parts of the silicon wafer we do not want etched.

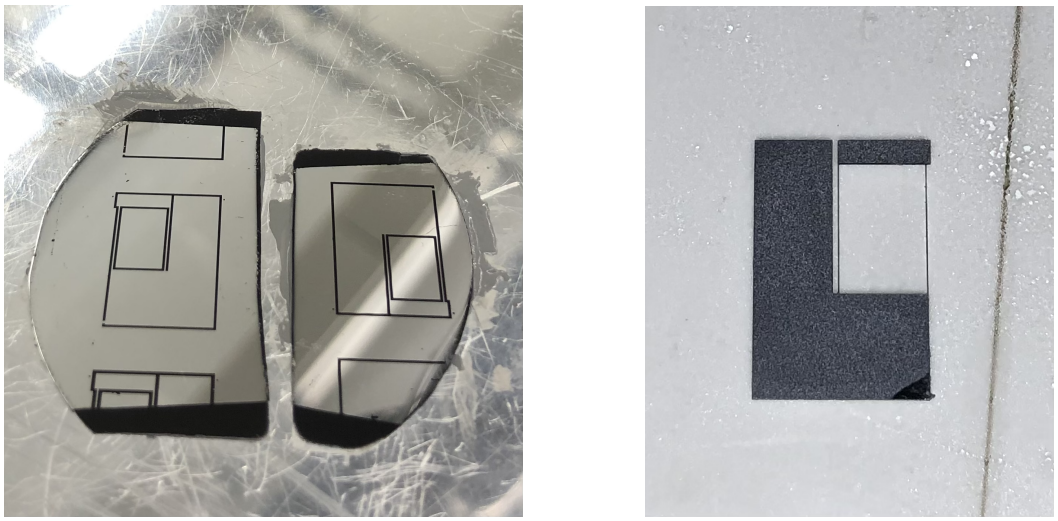

(a) (b)

Figure 5: (a) The parallelogram resonator pattern is stamped, developed, and has had the aluminum etched away on the patterned sections on two pieces of cut 280 μm silicon wafer. (b) The patterned parallelogram resonator is etched thoroughly through the Cryo-Si process.

The fabrication of the pendulum resonator from a 380 μm wafer is currently being tested. During our fabrication process so far on the 380 μm wafer, we have come across issues with the heat sink paste we use to keep thermal conduction. As our etch is ongoing the etch channels on the pattern seem to have a much slower rate than expected. Since the rate of etching is so slow, the heat sink paste has been able to go through the

small pieces of the resonator that are fully etched, causing the two walls around the spaces to be stuck together as seen in Figure 6b and hard to clean or tell if our resonator is etching through or if the paste is causing the etch to not be as effective. Using the heat sink paste has also brought up issues with cleaning the resonators thoroughly once they are fabricated without breaking them. We will aim to overcome issues with the heat sink paste by applying a thin layer of aluminum beneath the silicon to act as a barrier between the heat sink paste and silicon while still maintaining thermal conduction.

Since this resonator moves linearly and has the left and right sides of the test mass surrounded by the flexures, we will not be able to etch the v-grooves into the structure itself as the flexures would block the fibers from facing each other. Instead, we will be forming a v-groove on top of the structure using two bare fibers glued together.

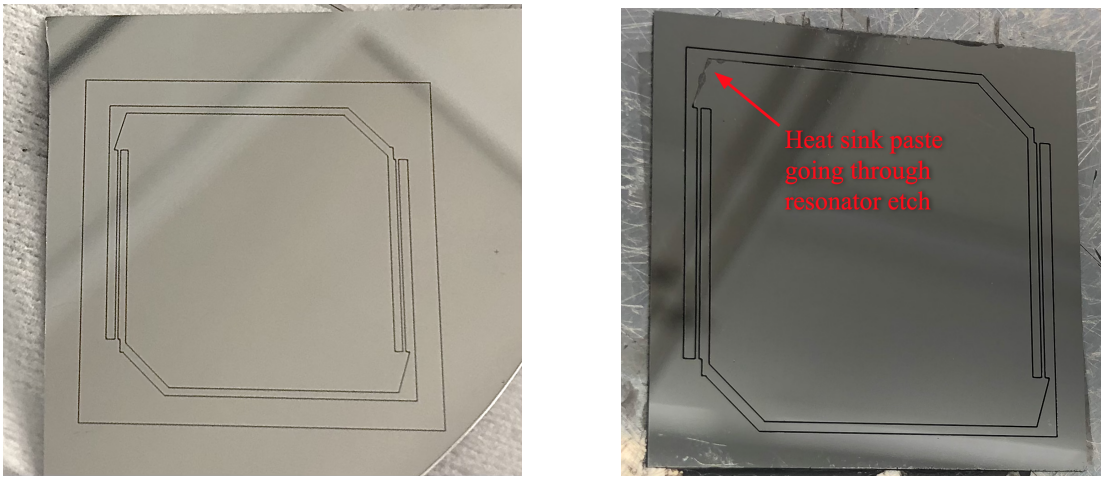

(a) (b)

Figure 6: (a) The pendulum resonator pattern is stamped, developed, and has had the aluminum etched away on the patterned sections on two pieces of cut 280 μm silicon wafer. (b) The Cryo-Si etch process has been ongoing on the substrate, though we have issues with the heat sink paste going through the etched parts of the silicon and causing the resonator to stick to itself.

Thicker silicon wafers will allow us to achieve higher sensitivities and larger mQ products. We plan to test the fabrication characteristics needed to fabricate such devices in the future.

4. RESONATOR CHARACTERIZATION AND OPTICAL READ-OUT

A Fabry-Pérot (FP) Cavity formed between the tips of two fibers is used to measure the experimental resonant frequency, Q-factor, and motion of the test mass. Since the pendulum resonator is fabricated from a single silicon wafer, the test mass and flexures need to be suspended so that they can move freely. We designed a mount made of aluminum which consists of threaded holes along the inner perimeter for the placement of steel alloy ball bearings that will run along the outside frame of the pendulum resonator, elevating the pendulum resonator into the air, such that the test mass and flexures can move freely as seen in Figure 7 The mount includes slots around each side so it can be screwed into the surface it will sit on, as well as windows around the sides for easier access to the resonator's sides.

The FP cavity is formed between the tips of two single-mode optical fibers cleaved at an angle less than or equal to 0.3°. The flat end of the fibers acts as mirrors that are parallel to the resonator. An input fiber is placed parallel to a secondary fiber that lies on the test mass. These fibers can be adjusted and held in place using v-grooves that are either etched into the resonator or formed on top of the resonator by gluing two bare fibers together. For a system with higher finesse, high reflectivity (HR) coating can be applied to the fiber tips, otherwise, a low finesse system is created as seen in Figure 8.

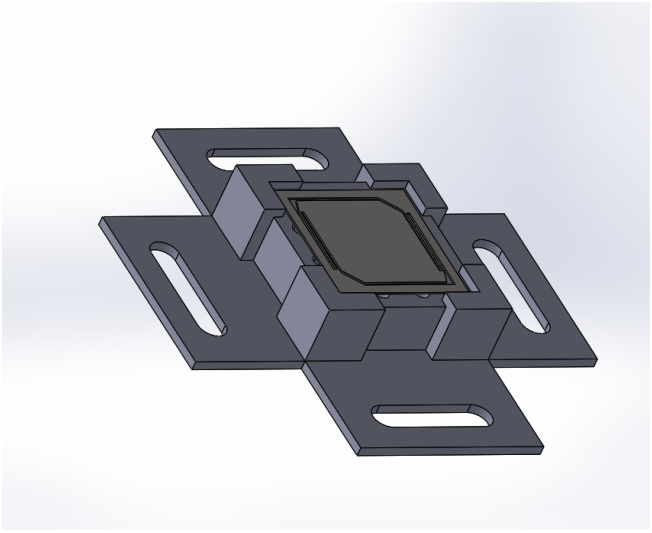

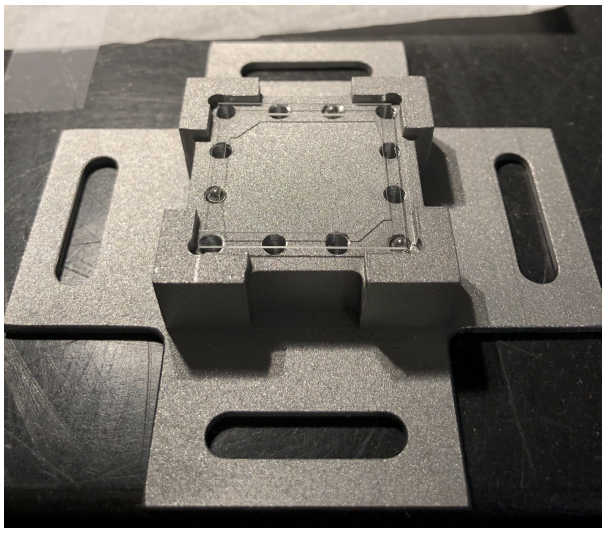

(a) (b)

Figure 7: (a) Solidworks drawing assembly of the mount for the pendulum resonator. (b) Aluminum mount with ball bearings installed and a sample resonator frame sitting on top of them.

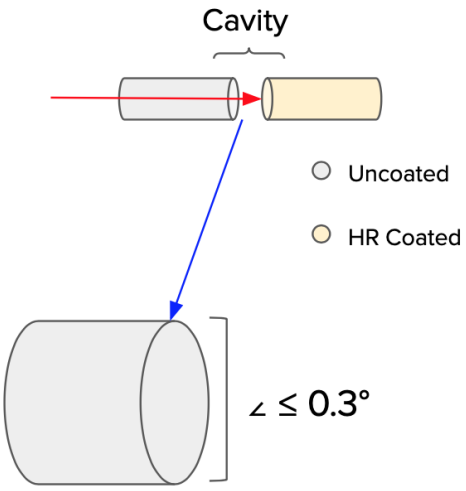

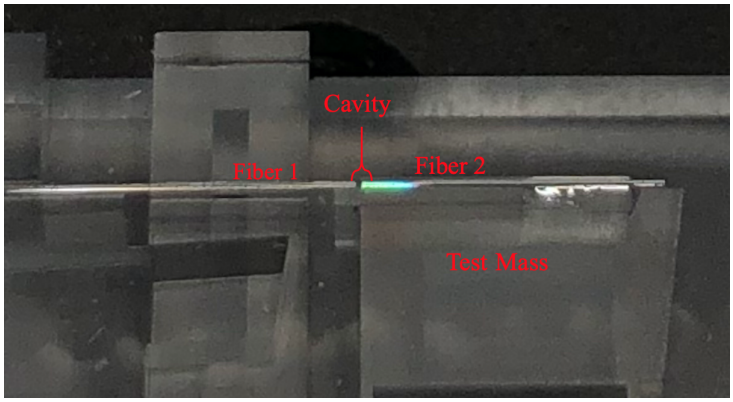

(a) (b)

Figure 8: (a) Two optical fibers cleaved at an angle less than or equal to 0.3° forming a cavity. The optical fibers can be coated to create a high-finesse system or uncoated to create a low-finesse system. (b) A cavity formed by two optical fibers, one with no HR coating and another with HR coating set up on one of our larger fused silica resonators.

The FP cavity readout method has been used in previous investigations with the larger fused silica resonators used in our lab[14,15] and will be implemented with the compact resonators. In Figure 9 a schematic of the system is shown. Laser light at 1550 nm is used in the system. The laser light goes through a fiber isolator which protects the laser from any reflected light. The laser light then moves into a 50/50 fiber coupler where one end goes to a primary photodetector for power normalization and the second end goes to an optical circulator. The optical circulator is used to further carry the laser light to the cavity formed between the tips of the two fibers and when there is reflected light the circulator will separate the reflected light from the input light and send it to a second photodetector for measurement.

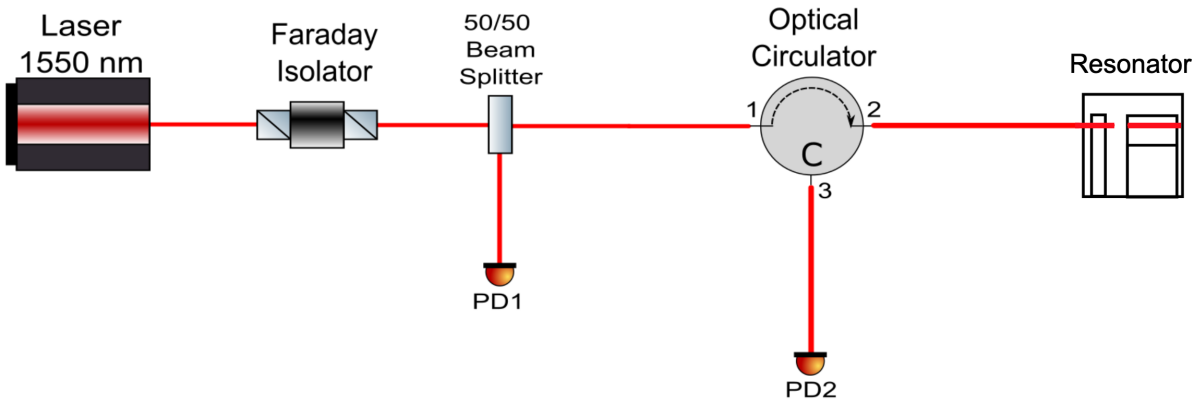

Figure 9: A schematic of the setup used to create a Fabry-Pérot system. Laser light is sent through an isolator followed by a 50/50 fiber split where one half goes through an optical circulator and the other half goes into the first photodetector for power normalization. The optical circulator carries the laser light to the resonator which is reflected back through the circulator and carried into the second photodetector which records the signal.

For a low finesse cavity, the voltage reflected from the cavity is proportional to the test mass motion:[14]

$$\delta V = \delta L \frac{\lambda_s}{L} \frac{\mathrm{d}V}{\mathrm{d}\lambda}\bigg|_{\lambda_s} \tag{1}$$

where λ_s is the laser's wavelength where the cavity sensitivity, $\mathrm{d}V/\mathrm{d}\lambda$, is maximized. L is the cavity length, which is in the order of 200 μm, and the voltage as a function of the wavelength is[14]

$$V(\lambda) = A\left(1 - \gamma \frac{1}{1 + \frac{\sin^2 \frac{2\pi L}{\lambda}}{\sin^2 \frac{\pi}{2\mathcal{F}}}}\right) \tag{2}$$

where A is the amplitude, γ is the cavity visibility, and $\mathcal{F}$ is the cavity's finesse. The voltage is converted to displacement and, finally, converted to acceleration using the mechanical resonator transfer function, which for $\omega < \omega_0$ is simply $\delta a = \omega_0^2 \delta x$. Previous work[15] using low finesse cavities, $\mathcal{F}$=2, has shown displacement noise levels between 10^{-12} and $10^{-13}\,\mathrm{m}/\sqrt{\mathrm{Hz}}$ at frequencies around 10 Hz.[15] These noise levels translate to acceleration noise levels between 10^{-7} and $10^{-8}\,\mathrm{m/s^2}/\sqrt{\mathrm{Hz}}$ for the pendulum resonator. For the parallelogram resonator, the acceleration noise levels are between 4×10^{-5} and $4 \times 10^{-6}\,\mathrm{m/s^2}/\sqrt{\mathrm{Hz}}$. Higher displacement sensitivity can be achieved by using high reflectivity coatings on the tips of the fibers and cavity resonance frequency tracking techniques.

5. SUMMARY

This paper discussed the design and fabrication of two silicon compact optomechanical resonators, and the foreseen optical read-out to measure the motion of the test masses. Silicon is the material chosen for the

resonator since it exhibits a high Q-value, and thus reduces the thermal noise limit, at low temperatures, as opposed to fused silica that drops rapidly below 250 K. The theoretical values for the $30\,\text{mm}\times30\,\text{mm}\times380\,\mu\text{m}$ pendulum resonator indicate a fundamental resonant mode at 52.4 Hz and Q-value of 4.3×10^5. The theoretical values for the $15\,\text{mm}\times10\,\text{mm}\times280\,\mu\text{m}$ parallelogram resonator are 1 kHz and Q-value of 3.1×10^5.

Regarding the fabrication of the two designs, we successfully fabricated two parallelogram resonators, while the fabrication of our pendulum resonator is being optimized. We will be further developing the fabrication process of the resonators to include the etching of v-grooves on the surfaces such that fiber-based optical cavities can be *easily* installed.

ACKNOWLEDGMENTS

The authors acknowledge financial support from the National Science Foundation (NSF) PHY-2045579.

REFERENCES

[1] Valdes, G., Hines, A., Nelson, A., Zhang, Y., and Guzman, F., "A characterization method for low-frequency seismic noise in ligo," *Applied Physics Letters* **121**(23), 234102 (2022).

[2] Akutsu, T., collaboration, K., et al., "Large-scale cryogenic gravitational-wave telescope in japan: Kagra," in [*Journal of Physics: Conference Series*], **610**(1), 012016, IOP Publishing (2015).

[3] Hines, A., Richardson, L., Wisniewski, H., and Guzman, F., "Optomechanical inertial sensors," *Applied optics* **59**(22), G167–G174 (2020).

[4] Nawrodt, R., Zimmer, A., Koettig, T., Schwarz, C., Heinert, D., Hudl, M., Neubert, R., Thürk, M., Nietzsche, S., Vodel, W., et al., "High mechanical q-factor measurements on silicon bulk samples," in [*Journal of Physics: Conference Series*], **122**(1), 012008, IOP Publishing (2008).

[5] Spear, B., "James watt: The steam engine and the commercialization of patents," *World Patent Information* **30**(1), 53–58 (2008).

[6] Blair, D. G., Liu, J., Moghaddam, E. F., and Ju, L., "Performance of an ultra low-frequency folded pendulum," *Physics Letters A* **193**(3), 223–226 (1994).

[7] Bertolini, A., DeSalvo, R., Fidecaro, F., Francesconi, M., Marka, S., Sannibale, V., Simonetti, D., Takamori, A., and Tariq, H., "Mechanical design of a single-axis monolithic accelerometer for advanced seismic attenuation systems," *Nuclear Instruments and Methods in Physics Research Section A: Accelerators, Spectrometers, Detectors and Associated Equipment* **556**(2), 616–623 (2006).

[8] Bertolini, A., DeSalvo, R., Fidecaro, F., and Takamori, A., "Monolithic folded pendulum accelerometers for seismic monitoring and active isolation systems," *IEEE transactions on geoscience and remote sensing* **44**(2), 273–276 (2006).

[9] Guzman, F., Kumanchik, L. M., Spannagel, R., and Braxmaier, C., "Compact fully monolithic optomechanical accelerometer," (2018).

[10] Nelson, A. and Guzman, F., "Micro-fabrication of si-based optomechanical inertial sensors for cryogenic temperatures," in [*Applied Optical Metrology IV*], **11817**, 78–83, SPIE (2021).

[11] Nelson, A. and Guzman, F., "Compact optomechanical inertial sensors with fused silicia and si-based resonators," in [*Optical and Quantum Sensing and Precision Metrology II*], **12016**, 91–96, SPIE (2022).

[12] Shapiro, B., Adhikari, R. X., Aguiar, O., Bonilla, E., Fan, D., Gan, L., Gomez, I., Khandelwal, S., Lantz, B., MacDonald, T., et al., "Cryogenically cooled ultra low vibration silicon mirrors for gravitational wave observatories," *Cryogenics* **81**, 83–92 (2017).

[13] Schnabel, R., Britzger, M., Brückner, F., Burmeister, O., Danzmann, K., Duck, J., Eberle, T., Friedrich, D., Luck, H., Mehmet, M., Nawrodt, R., Steinlechner, S., and Willke, B., "Building blocks for future detectors: Silicon test masses and 1550 nm laser light," *Journal of Physics: Conference Series* **228**, 012029 (may 2010).

[14] Guzmán Cervantes, F., Kumanchik, L., Pratt, J., and Taylor, J. M., "High sensitivity optomechanical reference accelerometer over 10 khz," *Applied Physics Letters* **104**(22), 221111 (2014).

[15] Guzman, F., Kumanchik, L. M., Spannagel, R., and Braxmaier, C., "Compact fully monolithic optomechanical accelerometer," *arXiv preprint arXiv:1811.01049* (2018).